

Correlations in suspensions confined between viscoelastic surfaces: Noncontact microrheology

Chen Bar-Haim* and Haim Diamant†

Raymond & Beverly Sackler School of Chemistry, Tel Aviv University, Tel Aviv 6997801, Israel

(Dated: September 13, 2017)

We study theoretically the velocity cross-correlations of a viscous fluid confined in a slit between two viscoelastic media. We analyze the effect of these correlations on the motions of particles suspended in the fluid. The compliance of the confining boundaries gives rise to a long-ranged pair correlation, decaying only as $1/r$ with the interparticle distance r . We show how this long-ranged effect may be used to extract the viscoelastic properties of the confining media without embedding tracer particles in them. We discuss the remarkable robustness of such a potential technique with respect to details of the confinement, and its expected statistical advantages over standard two-point microrheology.

I. INTRODUCTION

Most fluids and soft materials around us—e.g., suspensions, gels, biomaterials—are complex, having intrinsic time and length scales which are intermediate between the molecular and the macroscopic ones [1, 2]. The standard method to characterize the mechanical response of such materials, using macroscopic rheometers [3], has been supplemented in the past two decades by *microrheology* [4, 5]. In this technique the dynamics of tracer particles embedded in the complex medium is used to infer the response, i.e., the medium’s viscoelastic, frequency-dependent shear modulus $G(\omega)$ [6]. This can be done either actively, driving the particles by an external force, or passively, tracking their thermal fluctuations.

A particularly reliable variant of microrheology is *two-point microrheology* [5, 7], in which one tracks the correlated displacements of two particles as a function of their mutual distance r . Conservation of momentum in the medium guarantees that, at sufficiently large r , velocity correlations between two points in the medium must decay as $1/[G(\omega)r]$ [6, 8]. As a result, so do the correlations between the displacements of two well-separated particles inside the medium. Although it is insensitive to local details, unlike its one-point counterpart [7–9], two-point microrheology has not been widely used. The main reason is that it requires a large amount of statistics to be acquired over a limited time window, such that the mutual distance does not change appreciably during the measurement. In addition, passive microrheology is inapplicable in overly stiff media, where the thermal fluctuations of the tracer particles are suppressed.

Suspensions confined between solid boundaries, as in microfluidic channels, have been thoroughly studied in the past decade (see, e.g., Ref. [10] and references therein). Of particular relevance to the present work is the case of a quasi-two-dimensional (quasi-2D) layer of colloid particles confined between two planar surfaces

(see, e.g., [11–14]). With a few exceptions [15, 16], these studies have considered confining surfaces that can be assumed indefinitely rigid, such as glass plates. In this limit the fluid loses its momentum through friction with the rigid boundaries and, as a result, the correlations between confined particles are suppressed. The suppression, however, is found to be weaker than what one would expect—instead of the $1/r$ spatial decay mentioned above, the pair-correlations in these quasi-2D suspensions decay as $1/r^2$. This modified power law (rather than an exponential cutoff) originates in the conservation of fluid mass [10, 11].

One of our goals is to study what happens to the correlations in confined fluids and suspensions once the infinite-rigidity assumption is relaxed, and the boundaries are allowed to respond elastically or viscoelastically. The second goal is to examine whether the boundary-induced correlations could be used for a new type of “non-contact” two-point microrheology, where one would track the correlated motions of particles immersed in the confined fluid rather than the confining media. The concept of noncontact microrheology has been introduced in the context of interfacial layers, using one-point microrheology [17, 18] and atomic force microscopy [19]. As will be shown below, utilizing the distinct properties of quasi-2D suspensions confined between two compliant plates should make noncontact microrheology applicable to a broad class of soft materials.

The article is organized as follows. After presenting the model in Sec. II, we divide the analysis into two parts. The first (Sec. III) concerns the flow response of the confined fluid, in the absence of particles, to a localized impulse. In the second part (Sec. IV) we study the consequences of this response for the displacement correlations between particles embedded in the confined fluid. Finally, in Sec. V, we discuss the findings and their implications for noncontact two-point microrheology.

* chenbar@tau.ac.il

† hdiamant@tau.ac.il

II. MODEL

We consider a slit of thickness h , filled with an incompressible viscous fluid of viscosity η . The slit is bounded by two semi-infinite viscoelastic media, occupying the regions $z < -h/2$ and $z > h/2$. A pair of particles of radius a are embedded in the confined fluid, their centers separated by the vector \mathbf{r} . See the schematic illustration in Fig. 1. For simplicity we assume that the viscoelastic media are identical, having the same shear modulus $G(\omega)$, and that their frequency-dependent response is fully captured by this modulus [6] (in particular, inertia is negligible). Two additional assumptions are employed. (a) We focus on distances much larger than the slit thickness, $r \gg h > 2a$. (b) The flow of the confined fluid is assumed inertia-less (zero Reynolds number). For the present system, the latter assumption implies that the relaxation time required for fluid momentum to diffuse to the bounding surfaces, $h^2\rho/\eta$ (ρ being the fluid mass density), is negligibly small compared to the examined time scale ω^{-1} . For water in a micron-wide slit this inertial relaxation time is of the order of microseconds.

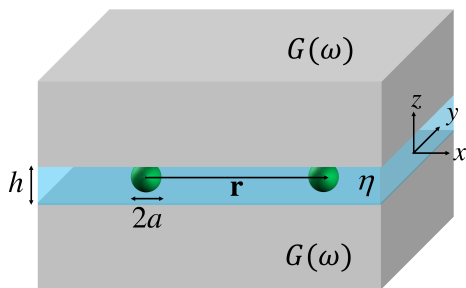


FIG. 1. Schematic view of the system and its parameters.

III. RESPONSE OF THE CONFINED FLUID

In the first part of the analysis we consider a particle-free confined fluid and study its flow response to a point impulse.

We begin with a heuristic account. Consider a localized oscillatory force $F \cos(\omega t)$, applied at a point in the fluid. The fluid-solid contact and the solid's response allow the stress to propagate in three dimensions while conserving momentum. Imagine a spherical envelope of radius r around the force. For $r \gg h$ the portion of envelope lying within the fluid-filled slit is negligible. The solid's displacement far away then decays as $u \sim F/(Gr)$ to guarantee that the stress (momentum flux) $\sigma \sim G\nabla u \sim F/r^2$, once integrated over the envelope, equal the momentum source F for any choice of r . Back in the confined fluid, due to the solid-fluid interface, this induces a flow velocity $v \sim \omega u \sim \omega F/(Gr)$. Thus, at large distances, the confined fluid has a velocity response that scales as $(\omega/G)/r$, independent of the

slit details. This response vanishes for an infinitely rigid solid ($G \rightarrow \infty$) and under steady forcing ($\omega \rightarrow 0$).

We now turn to a more detailed analysis. The two assumptions mentioned in Sec. II—lateral distances much larger than the slit thickness, and negligible relaxation time across that thickness—allow us to use an effective 2D model for the confined fluid. This so-called *lubrication approximation* [20, 21] is obtained by integration of the various variables over the thin dimension $z \in (-h/2, h/2)$. The resulting reduced hydrodynamic equations are

$$-\nabla p + \eta h \nabla^2 \mathbf{v} - \Gamma (\mathbf{v} - \dot{\mathbf{u}}) + \mathbf{f} = 0, \quad (1)$$

$$\nabla \cdot \mathbf{v} = 0, \quad (2)$$

expressing balance of forces (Eq. (1)) and incompressibility (Eq. (2)) of the quasi-2D flow. The following 2D fields, which are functions of lateral position $\mathbf{r} = (x, y)$ and time t , have been introduced: the flow velocity $\mathbf{v}(\mathbf{r}, t)$, fluid pressure $p(\mathbf{r}, t)$, surface displacement of the confining media at the slit boundaries $\mathbf{u}(\mathbf{r}, t)$, and an external force density $\mathbf{f}(\mathbf{r}, t)$, applied on the fluid parallel to the (x, y) plane. The symbols ∇ and $(\dot{\cdot})$ denote a 2D gradient and a time derivative.

A friction term, with a friction coefficient Γ , appears in the force balance, Eq. (1), characterizing the momentum exchange between the fluid and the confining media. To keep the analysis as general as possible, we do not specify Γ . This parameter depends on details of the flow profile in the z direction, created in the slit by \mathbf{f} , in particular, the boundary conditions at the fluid-solid interfaces. For example, in the simplest case of static no-slip boundary conditions at flat surfaces and a parabolic velocity profile (Poiseuille flow), we have $\Gamma = \eta/(12h)$ [22]. If out-of-plane boundary deformation is included in these boundary conditions, the integration over the thin dimension may yield Γ which is also time-dependent, turning the friction term in Eq. (1) into a convolution over time. From now on we Fourier-transform all functions from the time domain to the frequency domain, $t \rightarrow \omega$. Accordingly, the coefficient Γ appearing in the derivation below can be considered a frequency-dependent function, $\Gamma(\omega)$, without loss of generality.

Our aim now is to find the velocity response of the quasi-2D fluid, i.e., the Green's function $\mathcal{G}^f(\mathbf{r}, \omega)$ connecting the force density at point \mathbf{r}' with the flow velocity at point \mathbf{r} according to $v_i(\mathbf{r}, \omega) = \int d^2r' \mathcal{G}_{ij}^f(\mathbf{r} - \mathbf{r}', \omega) f_j(\mathbf{r}', \omega)$. To calculate it we need the solid's response as well, since the two are coupled. [See the frictional coupling to \mathbf{u} in Eq. (1).] The calculation is done through the following sequence of five logical steps. (i) A 2D force density \mathbf{f} is applied in the fluid. (ii) It results in the yet-unknown 2D flow velocity \mathbf{v} (the goal of the calculation) following Eqs. (1) and (2). (iii) Given a yet-unknown surface displacement \mathbf{u} , a friction force per unit area, $\Gamma(\mathbf{v} - \dot{\mathbf{u}})$, is applied on the surfaces. (iv) The solid responds to this surface force by a 3D displacement field, whose value at the surface is \mathbf{u} ; thus, once the solid

response has been dealt with, one obtains a relation between \mathbf{v} and \mathbf{u} . (v) This relation is substituted back in the flow equations (1) and (2) to obtain \mathbf{v} (and \mathbf{u} if so desired).

To account for the solid's response, in principle, one should solve the appropriate viscoelastic equations, along with boundary conditions at the slit surfaces which will ensure the continuity of stress across the boundaries. However, the corresponding 3D equations and boundary conditions can both be bypassed using a Green's function formulation, which will connect the flow-induced friction force density mentioned above, $\mathbf{P}(\mathbf{r}', \omega)$, acting on each of the solid surfaces at some point \mathbf{r}' , with the surface displacement at point \mathbf{r} ,

$$u_i(\mathbf{r}, \omega) = \int d^2 r' \mathcal{G}_{ij}^s(\mathbf{r} - \mathbf{r}', \omega) P_j(\mathbf{r}', \omega). \quad (3)$$

This formulation allows us also to remain within the 2D-reduced description. The 3D Green's function for a point force exerted on the surface of a solid is calculated in Ref. [23]. Once specialized to forces and surface displacements parallel to the surface, it reduces to

$$\mathcal{G}_{ij}^s(\mathbf{r}, \omega) = \frac{1 - \nu}{2\pi G(\omega)r} \left(\delta_{ij} + \frac{\nu}{1 - \nu} \frac{r_i r_j}{r^2} \right), \quad (4)$$

where ν is the solid's Poisson ratio. In 2D Fourier space, $\mathbf{r} \rightarrow \mathbf{q}$,

$$\mathcal{G}_{ij}^s(\mathbf{q}, \omega) = \frac{1}{G(\omega)q} \left(\delta_{ij} - \nu \frac{q_i q_j}{q^2} \right). \quad (5)$$

For Eqs. (4) and (5) to properly describe a solid, we assume a finite shear modulus at steady state, $G(\omega = 0) > 0$.

In the 2D-reduced description, the only force exerted on the solid surfaces is the flow-induced friction appearing in Eq. (1). Thus, the force per unit area exerted on each of the two surfaces is

$$\mathbf{P} = -\frac{1}{2}\Gamma(i\omega\mathbf{u} - \mathbf{v}). \quad (6)$$

Using this surface force in Eqs. (1)–(5) and solving for \mathbf{v} while considering a localized impulse in the fluid, $\mathbf{f}(\mathbf{r}, t) = \delta(\mathbf{r})\delta(t)$, we obtain the following expression for the fluid velocity response:

$$\mathcal{G}_{ij}^f(\mathbf{q}, \omega) = \frac{Gq + i\Gamma\omega/2}{q[G\eta hq^2 + \Gamma(G + i\eta\omega hq/2)]} \left(\delta_{ij} - \frac{q_i q_j}{q^2} \right). \quad (7)$$

In the limit of $G \rightarrow \infty$ (infinitely rigid solid), as well as in the limit of $\omega \rightarrow 0$ (steady state), Eq. (7) reduces to the known large-distance response function of a fluid between two infinitely rigid walls [10], $\mathcal{G}_{ij}^f(\mathbf{q}) = (\eta h q^2 + \Gamma)^{-1}(\delta_{ij} - \hat{q}_i \hat{q}_j)$. Another instructive limit is $\Gamma \rightarrow \infty$, forcing the bounding surfaces to move together with the fluid. In this limit Eq. (7) becomes $\mathcal{G}_{ij}^f(\mathbf{q}) = (\eta h q^2 + 2qG/i\omega)^{-1}(\delta_{ij} - \hat{q}_i \hat{q}_j)$, reproducing the known result for

a membrane (of 2D viscosity ηh) embedded in a liquid (of viscosity $G/i\omega$) [24]. Equation (7) can be inverted back to real space, yielding a complicated expression. In the limit of $r \gg h$ (which is anyhow demanded by the theory), we get

$$\mathcal{G}_{ij}^f(\mathbf{r}, \omega) = -\frac{1}{2\pi\Gamma r^2} \left(1 + \frac{\Gamma\eta h\omega^2}{4G^2} \right) \left(\delta_{ij} - 2\frac{r_i r_j}{r^2} \right) + \frac{i\omega}{4\pi G r} \frac{r_i r_j}{r^2}. \quad (8)$$

Equation (8), describing the spatio-temporal response of the quasi-2D fluid, is one of our central results. Its two terms reflect the two conservation laws at play. The first, decaying as $1/r^2$ and having a 2D-dipolar form, arises from mass conservation of the fluid, i.e., the response to the effective 2D mass dipole created by the confined localized force [10]. The flow lines produced by this term are depicted in Fig. 2(a). The second term, decaying as $1/r$, reflects momentum conservation of the entire system, i.e., the response to the 3D momentum monopole created by \mathbf{f} . The angular form of this term is dictated by the incompressibility of the flow, $\partial_i(r_i r_j/r^3) = 0$. The corresponding flow field is shown in Fig. 2(b). Figure 2(c) shows the combination of the two flow fields, with the dipolar component dominating at shorter distances (yet larger than h), and the monopolar one being dominant at the larger distances. The crossover between these two regions occurs around the frequency-dependent distance $\ell_c \sim G/(\omega\Gamma) \sim [G/(\eta\omega)]h$. With decreasing frequency, the crossover distance increases until, at steady state ($\omega = 0$), it becomes indefinitely large. In this long-time limit we are left with the mass-dipole response alone, as is known for quasi-2D fluids confined between infinitely rigid surfaces [11]. More precisely, this limit is obtained for $\omega \ll G/\eta$; for such low frequencies the solid deformation rate is too small to significantly affect the flow. Conversely, for frequencies higher than this value, the viscoelastic contributions to the fluid response become significant. Apart from the crossover arising from the last term of Eq. (8), the equation contains a smaller viscoelastic correction to the $1/r^2$ term, of order $(\omega\eta/G)^2$, which is of lesser significance for the following discussion.

Equation (8) also gives immediately, through the fluctuation-dissipation theorem, the cross-correlations between the flow velocities at two points separated by \mathbf{r} ,

$$C_{ij}(\mathbf{r}, \omega) \equiv \langle v_i(\mathbf{0}, \omega) v_j(\mathbf{r}, -\omega) \rangle = k_B T \mathcal{G}_{ij}^f(\mathbf{r}, \omega), \quad (9)$$

where $k_B T$ is the thermal energy.

IV. DISPLACEMENT CORRELATIONS OF EMBEDDED PARTICLES

We now turn to the consequences of the fluid response found in the preceding section for the dynamics of particles embedded in the fluid. In two-point microrheology

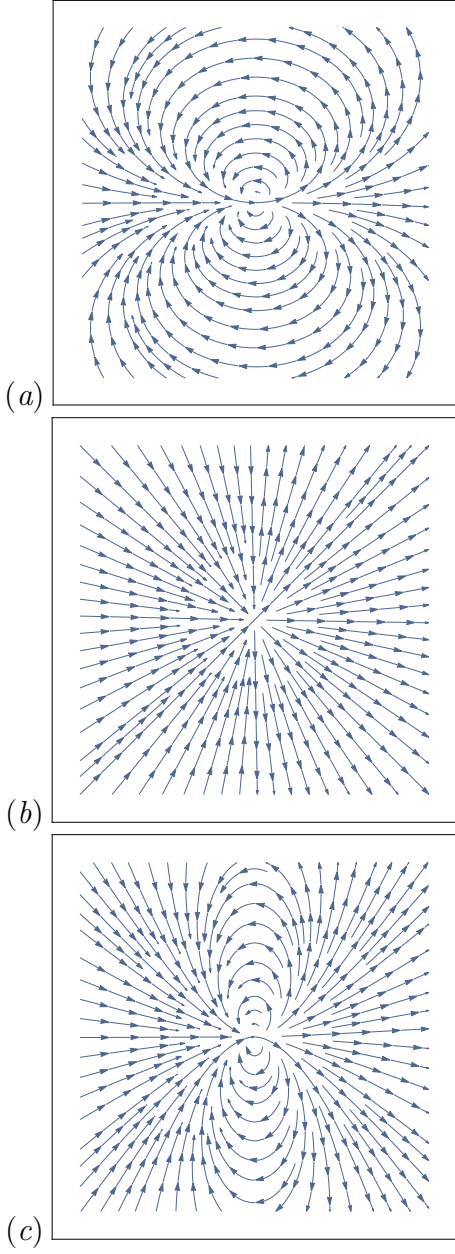


FIG. 2. 2D flow fields in the confined fluid, arising from a point impulse, $\mathbf{f} = f\hat{\mathbf{x}}$. (a) Monopolar term. (b) Dipolar term. (c) Total flow field.

one measures the cross-correlations between the displacements of two tracer particles, $\Delta\mathbf{R}^{(1)}(t)$ and $\Delta\mathbf{R}^{(2)}(t)$, whose positions are separated by \mathbf{r} , during the time interval t , $D_{ij}(\mathbf{r}, t) \equiv \langle \Delta R_i^{(1)}(t) \Delta R_j^{(2)}(t) \rangle$. They are conventionally decomposed into a longitudinal correlation and a transverse one, where the displacements are projected on, and perpendicular to, the separation vector \mathbf{r} . Assuming that the pair separation is much larger than the particle radius a , $r \gg a$, the particles' displacement correlations are obtained from the fluid's velocity correlations through a double time integration, or, in the

frequency domain,

$$D_{\parallel}(r, \omega) = -\frac{2}{\omega^2} C_{xx}(r\hat{\mathbf{x}}, \omega) \quad (10)$$

$$= -\frac{k_B T \alpha h}{\pi \eta \omega^2} \left(1 + \frac{\eta^2 \omega^2}{4 \alpha G^2} \right) \frac{1}{r^2} + \frac{k_B T}{2 \pi i \omega G} \frac{1}{r},$$

$$D_{\perp}(r, \omega) = -\frac{2}{\omega^2} C_{xx}(r\hat{\mathbf{y}}, \omega) \quad (11)$$

$$= \frac{k_B T \alpha h}{\pi \eta \omega^2} \left(1 + \frac{\eta^2 \omega^2}{4 \alpha G^2} \right) \frac{1}{r^2}.$$

In Eqs. (10) and (11) we have introduced a dimensionless coefficient, α , relating the friction coefficient Γ to the actual system's parameters according to $\Gamma^{-1} = \alpha h / \eta$. It depends on the degree of particle confinement, a/h , and the boundary conditions at the fluid-solid interfaces. Once again, we prefer to remain on the most general level and regard it as a phenomenological parameter to be determined by experiment or a more detailed calculation for a specific system. We note, however, that the value of α is typically small and depends weakly on a/h . For pointlike particles and no-slip boundary conditions, one has $\alpha(a/h \rightarrow 0) \simeq 0.030$ [25], decreasing for larger confinement ratio to $\alpha(a/h \simeq 0.45) \simeq 0.019$ [26]. (For no-slip boundary conditions α vanishes for $a/h = 1/2$, as the sphere touches the walls.)

Equations (10) and (11) contain our main experimental predictions. They can be used to extract the viscoelastic shear modulus $G(\omega)$ of the confining media from the displacement correlations of particles lying *outside of them*, inside the confined viscous fluid. Since only shear stresses are exerted on the boundaries, Eqs. (10) and (11) are independent of the Poisson ratio and thus cannot be used to measure it. (The main ingredient of most soft materials, anyway, is a molecular solvent, making them nearly incompressible, with $\nu \simeq 1/2$.) The dependencies of the longitudinal and transverse displacement correlations on the distance between the two particles (for a given frequency) are presented in Fig. 3(a). As seen in Eqs. (10) and (11), and as was observed experimentally for rigid plates [11], the $1/r^2$ terms have opposite signs in the two correlations. This is a result of the dipolar shape of the underlying response (see Fig. 2(a)). While the transverse correlation contains only this contribution for $r \gg h$, the longitudinal one crosses over around $\ell_c \sim [\alpha G / (\eta \omega)] h$ to the $1/r$ monopolar term. (As noted above, the absence of the $1/r$ term in D_{\perp} is dictated by the incompressibility of the flow.) Moreover, the particular spatial decays of the two correlations can be exploited to isolate the monopolar, viscoelastic contribution,

$$\bar{D}(r, \omega) \equiv D_{\parallel}(r, \omega) + D_{\perp}(r, \omega) = \frac{k_B T}{2 \pi i \omega G} \frac{1}{r}. \quad (12)$$

This residual pair-correlation is shown in Fig. 3(b). Equation (12) might be the most useful result of this work. Adding up the two measured correlations is predicted to leave a residual long-range correlation, $\bar{D} \sim 1/r$, whose coefficient is inversely proportional to $G(\omega)$.

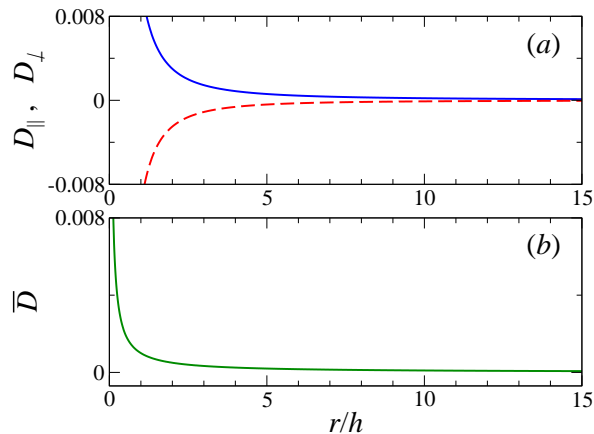


FIG. 3. Two-point displacement correlations, normalized by $-\pi\omega^2\eta h/k_B T$, as a function of particle separation, normalized by h . Once normalized, these functions depend only on the parameters $G/(\eta\omega)$ and α . We have used $G/(\eta\omega) = 500$ and $\alpha = 0.01$. Panel (a) shows the longitudinal (solid blue) and transverse (dashed red) correlations. Panel (b) presents the residual correlation obtained by adding together the two correlations of (a).

V. DISCUSSION

From the fundamental point of view, our findings indicate the existence of long-ranged correlations in confined fluids and between particles suspended in them. Not only do the steady-state correlations decay as $1/r^2$, as was found earlier for rigid slits [11–14], the compliance of the confining media leads to an even weaker spatial decay of the time-dependent correlations, falling off as $1/r$. In addition to the pair-correlations analyzed here, these long-ranged effects should influence the collective dynamics of suspensions confined in soft materials, which calls for further study.

From the practical perspective, the measurable correlation defined in Eq. (12) suggests a noncontact, two-point, microrheological technique of several key advantages. (i) While the signal \bar{D} should not be weaker than the one used in standard two-point microrheology, which also scales as $k_B T/(\omega G r)$ [7], it is extracted from the much stronger fluctuations of particles suspended in a viscous fluid. (ii) Arising from the conservation of momentum in the entire 3D system, it is guaranteed to be the only correlation term remaining at sufficiently large

distances. (iii) For the same reason, it is independent of details of the confining slit, such as its width h and coefficient α . Thus, in principle, one does not have to measure these parameters before using \bar{D} to extract G . (iv) Furthermore, the residual correlation should be robust also against modifications of the confining surfaces; one can coat the surfaces with thin layers of different composition so long as their thickness is much smaller than the sampled lateral distances. (v) All particles in the slit can be imaged on the focal plane. (vi) Since large-distance pair correlations in the confined suspension are practically independent of concentration [26], one can use dense suspensions to improve the statistics. Indeed, two-point correlations in quasi-2D suspensions confined between two rigid surfaces have been measured with remarkable accuracy over distances more than ten times larger than the confinement width h [11, 26].

At the same time, in practice, one cannot expect exact mutual cancellation of the $\pm 1/r^2$ terms in the measured D_{\parallel} and D_{\perp} . For example, assuming noise of a few percent in the measurements, we need the $1/r$ term to be larger than a few percent of the $1/r^2$ term. This will occur at distances $r/h \gtrsim 10^{-2}\alpha[G/(\omega\eta)]$. An entangled F-actin network has $G/\omega \sim 1$ Pa·s over a frequency range of 1–100 Hz [9], yielding for confined water ($\eta = 10^{-3}$ Pa·s) a strong signal at all relevant distances. (Note that the small value of α helps the dominance of the $1/r$ signal.) In the case of stiffer materials, such as typical elastomers ($G \sim 1$ MPa), one would need higher frequencies, $\omega \gtrsim 1$ kHz (or time scales of order milliseconds), to observe a similar effect. Another experimental restriction is that the confining media should be much thicker than the largest lateral distance between tracked particles. Overall, for soft biomaterials, the main complication in applying the noncontact microrheology proposed here is expected to be the preparation of the required double-slab sample.

ACKNOWLEDGMENTS

We are grateful to Shigeyuki Komura for spotting an error in an earlier version of the article. We thank Yael Roichman for helpful discussions. This work has been supported by the Israel Science Foundation (Grant No. 164/14).

-
- [1] T. Witten, *Structured fluids* (Oxford university press, 2004).
 - [2] M. Doi, *Soft matter physics* (Oxford university press, 2013).
 - [3] R. Larson, *The Structure and Rheology of Complex Fluids* (Oxford University Press, New York, 1999).
 - [4] T. G. Mason and D. A. Weitz, Phys. Rev. Lett. **74**, 1250 (1995).

- [5] T. A. Waigh, Rep. Progr. Phys. **79**, 074601 (2016).
- [6] For brevity, as was done in earlier works, we use throughout the paper the same notation, $G(\omega)$, to denote both the complex frequency-dependent modulus, $G = G' + iG''$, and the one obtained from the real, time-dependent modulus $G(t)$ through a one-sided Fourier (equivalently, Laplace) transform. The meaning in each instance should be clear from the context.

- [7] J. C. Crocker, M. T. Valentine, E. R. Weeks, T. Gisler, P. D. Kaplan, A. G. Yodh, and D. A. Weitz, *Phys. Rev. Lett.* **85**, 888 (2000).
- [8] H. Diamant, *Eur. Phys. J. E* **38**, 32 (2015).
- [9] A. Sonn-Segev, A. Bernheim-Groswasser, H. Diamant, and Y. Roichman, *Phys. Rev. Lett.* **112**, 088301 (2014).
- [10] H. Diamant, *J. Phys. Soc. Jpn.* **78**, 041002 (2009).
- [11] B. Cui, H. Diamant, B. Lin, and S. A. Rice, *Phys. Rev. Lett.* **92**, 258301 (2004).
- [12] J. Santana-Solano, A. Ramírez-Saito, and J. L. Arauz-Lara, *Phys. Rev. Lett.* **95**, 198301 (2005).
- [13] S. Bhattacharya, J. Bławdziewicz, and E. Wajnryb, *Physica A* **356**, 294 (2005).
- [14] A. Alvarez and R. Soto, *Phys. Fluids* **17**, 093103 (2005).
- [15] A. Daddi-Moussa-Ider and S. Gekle, *J. Chem. Phys.* **145**, 014905 (2016).
- [16] A. Daddi-Moussa-Ider, A. Guckenberg, and S. Gekle, *Phys. Fluids* **28**, 071903 (2016).
- [17] R. Shlomovitz, A. A. Evans, T. Boatwright, M. Dennin, and A. J. Levine, *Phys. Rev. Lett.* **110**, 137802 (2013).
- [18] T. Boatwright, M. Dennin, R. Shlomovitz, A. A. Evans, and A. J. Levine, *Phys. Fluids* **26**, 071904 (2014).
- [19] N. Gavara and R. S. Chadwick, *Nat. Methods* **7**, 650 (2010).
- [20] O. Reynolds, *Phil. Trans. R. Soc. Lond.* **177**, 157 (1886).
- [21] A. Oron, S. H. Davis, and S. G. Bankoff, *Rev. Mod. Phys.* **69**, 931 (1997).
- [22] J. Happel and H. Brenner, *Low Reynolds Number Hydrodynamics* (Martinus Nijhoff, The Hague, 1983).
- [23] L. D. Landau and E. M. Lifshitz, *Theory of Elasticity*, 3rd ed. (Pergamon press, 1986).
- [24] S. Komura, S. Ramachandran, and K. Seki, *Europhys. Lett.* **97**, 68007 (2012).
- [25] N. Liron and S. Mochon, *J. Eng. Math.* **10**, 287 (1976).
- [26] H. Diamant, B. Cui, B. Lin, and S. A. Rice, *J. Phys. Condens. Matter* **17**, S4047 (2005).